JVSTB
JOURNAL OF VACUUM SCIENCE AND TECHNOLOGY B

Molecular beam epitaxy of highly mismatched N-rich GaN1−xSbx and InN1−xAsx alloys

Sergei V. Novikov, Kin M. Yu, Alejandro Levander, Douglas Detert, Wendy L. Sarney et al.

Citation: J. Vac. Sci. Technol. B **31**, 03C102 (2013); doi: 10.1116/1.4774028
View online: http://dx.doi.org/10.1116/1.4774028
View Table of Contents: http://avspublications.org/resource/1/JVTBD9/v31/i3
Published by the AVS: Science & Technology of Materials, Interfaces, and Processing

Molecular beam epitaxy of highly mismatched N-rich $GaN_{1-x}Sb_x$ and $InN_{1-x}As_x$ alloys

Sergei V. Novikov[a)]
School of Physics and Astronomy, University of Nottingham, Nottingham NG7 2RD, United Kingdom

Kin M. Yu
Materials Sciences Division, Lawrence Berkeley National Laboratory, 1 Cyclotron Road, Berkeley, California 94720

Alejandro Levander and Douglas Detert
Materials Sciences Division, Lawrence Berkeley National Laboratory, 1 Cyclotron Road, Berkeley, California 94720 and Department of Materials Science & Engineering, University of California, Berkeley, California 94720

Wendy L. Sarney
U.S. Army Research Laboratory, 2800 Powder Mill Road, Adelphi, Maryland 20783

Zuzanna Liliental-Weber
Materials Sciences Division, Lawrence Berkeley National Laboratory, 1 Cyclotron Road, Berkeley, California 94720

Martin Shaw and Robert W. Martin
Department of Physics, SUPA, University of Strathclyde, Glasgow G4 0NG, United Kingdom

Stefan P. Svensson
U.S. Army Research Laboratory, 2800 Powder Mill Road, Adelphi, Maryland 20783

Wladek Walukiewicz
Materials Sciences Division, Lawrence Berkeley National Laboratory, 1 Cyclotron Road, Berkeley, California 94720

C. Thomas Foxon
School of Physics and Astronomy, University of Nottingham, Nottingham NG7 2RD, United Kingdom

(Received 5 November 2012; accepted 14 December 2012; published 8 January 2013)

GaN materials alloyed with group V anions form the so-called highly mismatched alloys (HMAs). Recently, the authors succeeded in growing N-rich $GaN_{1-x}As_x$ and $GaN_{1-x}Bi_x$ alloys over a large composition range by plasma-assisted molecular beam epitaxy (PA-MBE). Here, they present first results on PA-MBE growth and properties of N-rich $GaN_{1-x}Sb_x$ and $InN_{1-x}As_x$ alloys and compare these with $GaN_{1-x}As_x$ and $GaN_{1-x}Bi_x$ alloys. The enhanced incorporation of As and Sb was achieved by growing the layers at extremely low growth temperatures. Although layers become amorphous for high As, Sb, and Bi content, optical absorption measurements show a progressive shift of the optical absorption edge to lower energy. The large band gap range and controllable conduction and valence band positions of these HMAs make them promising materials for efficient solar energy conversion devices. [http://dx.doi.org/10.1116/1.4774028]

I. INTRODUCTION

In order to effectively convert solar energy into electric power or any other form of usable energy, we need to develop novel semiconductor materials, which will absorb photons over the full solar energy spectrum. Our research concentrates on GaN materials alloyed with group V anions of very different size and electronegativity, the so-called highly mismatched alloys (HMAs). The electronic structures of the conduction and valence bands of HMAs in the dilute alloy limits have been well described by the band anticrossing (BAC) model.[1,2] For highly mismatched $GaN_{1-x}As_x$ alloys over the whole composition range, extrapolation of the BAC model predicts that the energy gap can have a wide range from 0.7 to 3.4 eV.[1] An even stronger modification of the band structures is anticipated for more extremely mismatched $GaN_{1-x}Sb_x$ and $GaN_{1-x}Bi_x$ alloys.[1–3] The large band gap range and controllable conduction and valence band positions of these HMAs make them promising materials for efficient solar energy conversion devices.[1–3] For example, theoretical calculations[1–3] predict that the addition of As or Sb to GaN at concentrations below about 10% can substantially lift the valence band edge and thus reduce the fundamental bandgap. The modification of the band structure enables the material to capture more photons from the solar spectrum while still maintaining the favorable band alignment of GaN with the Redox potential for spontaneous hydrogen production by water splitting. However, the synthesis of these alloys is difficult due to the large size/electronegativity mismatch between the anions.

Recently, we succeeded in growing $GaN_{1-x}As_x$ and $GaN_{1-x}Bi_x$ alloys over a large composition range by

a)Electronic mail: Sergei.Novikov@nottingham.ac.uk

plasma-assisted molecular beam epitaxy (PA-MBE).[4–7] The enhanced incorporation of As and Bi was achieved by growing the layers at extremely low growth temperatures. While $GaN_{1-x}As_x$ can be grown over the entire composition, $GaN_{1-x}Bi_x$ can only be achieved with a limited Bi incorporation of ~11% because of the larger degree of mismatch between N and Bi. Optical absorption measurements show a progressive shift of the optical absorption edge to lower energy as the As and Bi content increases. For example, despite the fact that $GaN_{1-x}As_x$ alloys become amorphous for $x > 0.1$, a downward shift of a well-developed optical band gap from ~3.4 eV in GaN to ~0.8 eV in $GaN_{0.2}As_{0.8}$ was observed. The results strongly suggest that amorphous $GaN_{1-x}As_x$ alloys have short-range order resembling random crystalline $GaN_{1-x}As_x$ alloys. The large band gap range of the amorphous $GaN_{1-x}As_x$ covers much of the solar spectrum making this material system a good candidate for full spectrum multijunction solar cells. The amorphous nature of the $GaN_{1-x}As_x$ alloys is particularly advantageous since low cost substrates such as glass can be used for solar cell fabrication.

In this paper, we present our first results on MBE growth and properties of N-rich $GaN_{1-x}Sb_x$ and $InN_{1-x}As_x$ alloys and compare these with $GaN_{1-x}As_x$ and $GaN_{1-x}Bi_x$ alloys. To our knowledge, these are the first experimental data on the growth of these N-rich alloys.

II. EXPERIMENT

The $GaN_{1-x}Sb_x$ and $InN_{1-x}As_x$ layers were grown by PA-MBE in a MOD-GENII system. Two-inch diameter sapphire and Pyrex substrates were used. The active nitrogen for the growth of the group III-nitrides was provided by an HD25 RF activated plasma source. Standard Veeco effusion sources were used for Ga, In, and Sb. We have used arsenic in the form of As_2 produced by a Veeco arsenic valved cracker. In order to increase uniformity across the wafer, all films were grown with substrate rotation of ~10 rpm. In MBE, the substrate temperature is normally measured using an optical pyrometer, however, because we have used uncoated transparent sapphire and Pyrex wafers, the pyrometer measures the temperature of the substrate heater, not that of the substrate. Therefore in this study, our estimates of the growth temperature are based on thermocouple readings.[6]

All of the $GaN_{1-x}Sb_x$ layers were grown on sapphire substrates. Prior to the growth of the $GaN_{1-x}Sb_x$ layers, we heated the sapphire wafers to ~700 °C and annealed them for 20 min. After annealing, the substrate was cooled down to the growth temperature over a 20 min period under a reduced active nitrogen flux and growth was initiated by simultaneously opening of the Ga and N shutters. The Sb shutter was opened after a 1 min delay in order to avoid the deposition of any Sb on the sapphire surface before GaN growth. The growth time was kept at 2 h for all layers. In our initial studies on $GaN_{1-x}Bi_x$, we have established that, in order to incorporate a significant amount of Bi in GaN, the MBE growth temperature needs to be very low.[6,7] Therefore, the majority of the $GaN_{1-x}Sb_x$ layers in this study were grown at low temperatures ~80–90 °C. However, we have also studied the deposition of $GaN_{1-x}Sb_x$ in a wide temperature range from ~500 °C down to room temperature.

It is now well established that there are three main regimes for PA-MBE growth of GaN (Ref. 8)—N-rich growth (here the active nitrogen flux is larger than the Ga-flux); Ga-rich growth (here the active nitrogen flux is less than the Ga-flux), and strongly Ga-rich growth (here the active nitrogen flux is much less than the Ga-flux and Ga droplets are formed on the surface). In our current studies, we have grown $GaN_{1-x}Sb_x$ layers under both N-rich and Ga-rich conditions and have also investigated the transition from N-rich to Ga-rich growth.

All the $InN_{1-x}As_x$ layers were grown on Pyrex substrates. Pyrex is not as thermally stable as sapphire; therefore, we did not use a high temperature annealing stage in the growth process. Prior to the growth of the $InN_{1-x}As_x$ layers, we heated the substrates to the desired growth temperatures and annealed them for 30 min. The growth was started by simultaneous opening of the In and N shutters. The As has been opened with a ~30 s delay in order to avoid deposition of any As on the substrate surface before InN growth. The growth time was 2 h for all layers.

Crystallinity of the grown layers was studied *in situ* using reflection high-energy electron diffraction (RHEED) and after growth *ex situ* measurements were performed using x-ray diffraction (XRD). We have studied Sb incorporation in $GaN_{1-x}Sb_x$ layers and As incorporation in $InN_{1-x}As_x$ using Rutherford backscattering spectrometry (RBS) with a 3.04 MeV He++ beam, secondary ion mass spectrometry (SIMS) using Cameca IMS-3F and IMS-4F systems, and by electron probe microanalysis (EPMA) using a Cameca SX100 apparatus. Microstructural information on the alloys was obtained by transmission electron microscopy (TEM) techniques. Microscopic crystallinity and phase separation were studied by directly comparing the selected area electron diffraction patterns and high resolution microscopy. The band gap of the thin films was measured by optical transmission and reflection using a Perkin Elmer Lambda 950 Spectrophotometer over the wavelength range of 190–3000 nm.

III. RESULTS AND DISCUSSION

Despite the extremely low growth temperatures, we observed polycrystalline growth for all undoped GaN layers by *in situ* RHEED during and after the growth. This was also confirmed by *ex situ* XRD studies, showing diffraction peaks normally associated with polycrystalline GaN with a strong preferential c-axis orientation along the growth direction. Polycrystalline growth was observed for the layers grown under both Ga-rich and N-rich conditions. However, even a small amount (beam equivalent pressure, BEP above 10^{-8} Torr) of Sb suppressed the crystallinity and the layers became amorphous as can be seen by *in situ* RHEED and *ex situ* XRD. Such behavior is very similar to the influence of As and Bi flux on the growth of GaN layers, that we have observed previously in epitaxy of $GaN_{1-x}As_x$ and $GaN_{1-x}Bi_x$ alloys by PA-MBE.[4–7]

We have studied the composition of the $GaN_{1-x}Sb_x$ layers using both RBS and EPMA. Figure 1(a) shows the RBS data for the Sb incorporation in $GaN_{1-x}Sb_x$ layers grown at ~80–90 °C under N-rich conditions. The Sb concentration increases linearly with the increase of the BEP of Sb. At the same time, we observed a gradual decrease in the Group III(Ga)/Group V(N plus Sb) concentration ratio from values slightly above 1 (stoichiometric material) to about 0.4 for a very high Sb content [Fig. 1(b)]. We note that the Ga-N bond (2.24 eV/bond[9]) is significantly stronger than the Ga-Sb bond (1.48 eV/bond[9]). It is therefore reasonable to assume that in off stoichiometric materials with III/V ratio <1, excess Sb atoms are present as Sb_{Ga} antisites and/or Sb clusters. In such situation, it is difficult to estimate the exact composition of the $GaN_{1-x}Sb_x$ alloys since some Sb atoms will not take part in the formation of the alloy. Therefore in Fig. 1(a), we presented the RBS measured Sb content as the Sb/Ga ratio. The composition of the $GaN_{1-x}Sb_x$ layers at the different Sb fluxes has also been confirmed by our EPMA studies.

Uniformity of the Sb incorporation in the $GaN_{1-x}Sb_x$ layers has been studied by SIMS. In order to detect Sb, both stable antimony isotopes ^{121}Sb and ^{123}Sb have been analyzed. We have no calibrated standards for the complicated Ga–N–Sb matrix and our SIMS results are presented in arbitrary units as shown in Fig. 2. We observed a uniform distribution of Sb inside the layers for the entire range of the Sb concentrations, in perfect agreement with our RBS measurements.

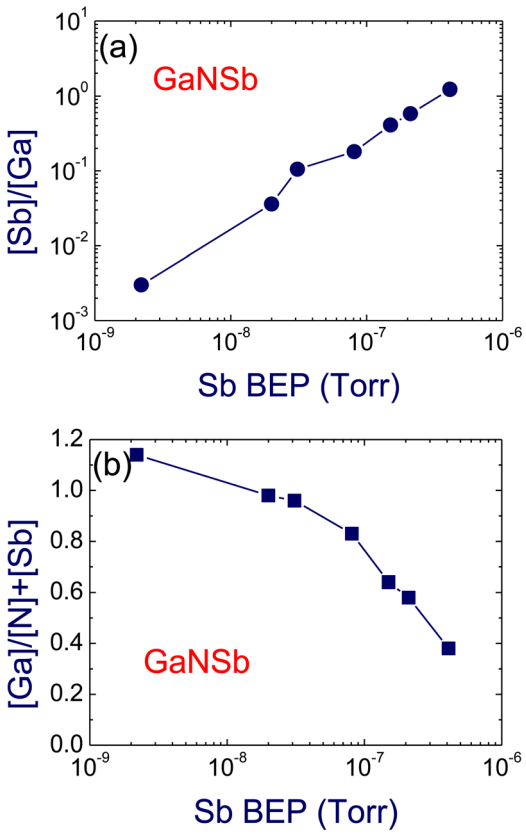

FIG. 1. (Color online) Sb/Ga (a) and Ga/(N + Sb) (b) concentration ratios in the GaNSb layers measured by RBS as a function of the Sb flux during PA-MBE.

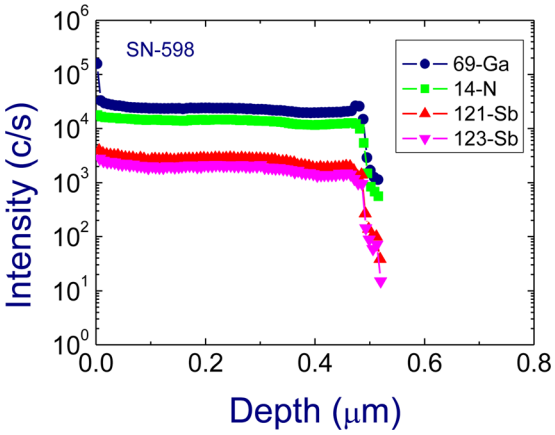

FIG. 2. (Color online) SIMS profile for Ga, N, and Sb at the center of a $GaN_{1-x}Sb_x$ layer.

Figure 3 presents a typical cross-sectional TEM micrograph of a $GaN_{1-x}Sb_x$ layer grown at ~80−90 °C and a high Sb flux. The layer is completely amorphous, as also indicated by the diffuse rings in the diffraction pattern (not shown). This is in strong contrast to the crystalline sapphire substrate, which can be seen at the bottom of the TEM figure.

Optical absorption and reflection measurements show a progressive shift of the optical band gap to lower energy with increase of the Sb incorporation in GaN layer. The square of the absorption coefficient $(\alpha^*h\upsilon)^2$ versus photon energy for $GaN_{1-x}Sb_x$ films grown at different Sb fluxes under N-rich conditions at ~80–90 °C is shown in Fig. 4. The direct band gap of the alloy can be estimated by extrapolating the linear part of the absorption edge down to the energy axis. The overall Sb compositions measured by RBS

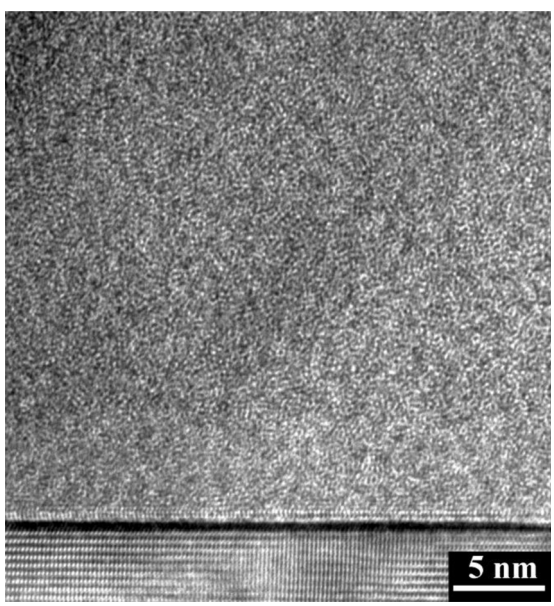

FIG. 3. Typical cross-sectional TEM micrograph of an amorphous $GaN_{1-x}Sb_x$ layer grown on sapphire at ~80–90 °C and a high Sb flux.

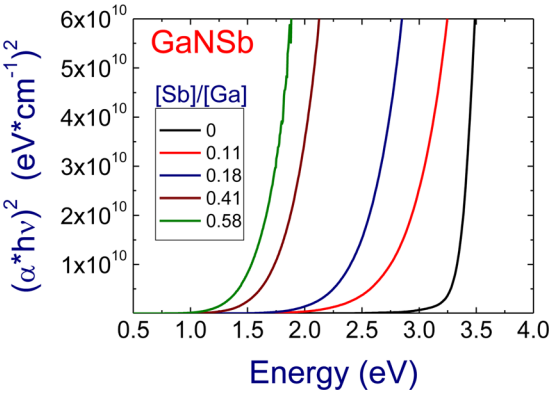

FIG. 4. (Color online) Energy dependence of the square of the absorption coefficient $(\alpha^*h\upsilon)^2$ for $GaN_{1-x}Sb_x$ layers, grown at different Sb fluxes.

are also given for all layers in the form of the Sb/Ga ratio. Figure 4 shows that despite the fact that $GaN_{1-x}Sb_x$ layers are amorphous, the energy gap decreases monotonically with increasing Sb content. The band gap decreased from ~3.4 eV for GaN layers up to ~1.3 eV for $GaN_{1-x}Sb_x$ layers with the highest Sb content.

This behavior of the optical properties of $GaN_{1-x}Sb_x$ layers is very similar to the optical properties of amorphous $GaN_{1-x}As_x$ alloys, where despite the fact that $GaN_{1-x}As_x$ layers are becoming amorphous at high As content, the energy gap decreases monotonically with increasing As concentration.[4,5] Theoretical predictions[1–3] suggest a more drastic decrease of the band gap with incorporation of Sb in GaN in comparison with As incorporation in GaN. Unfortunately, since the exact Sb content in the $GaN_{1-x}Sb_x$ alloy at this stage cannot be determined due to the presence of Sb_{Ga} antisites and/or Sb clusters, a direct comparison of measured and calculated bandgap cannot be done. However, we can definitely observe a gradual shift of the $GaN_{1-x}Sb_x$ band gap with increasing Sb incorporation. The results strongly suggest that amorphous $GaN_{1-x}Sb_x$ alloys have short-range order resembling random crystalline $GaN_{1-x}Sb_x$ alloys. The large band gap range of the amorphous $GaN_{1-x}Sb_x$ alloys covers much of the solar spectrum making this material system a good candidate for solar energy conversion devices.

In recent years, we have performed significant investigations on the growth and characterization of GaN-based HMAs.[4–7] In contrast, to the best of our knowledge no experimental data are available so far for InN-based highly mismatched alloys. Despite more than three decades of research, indium nitride (InN) remains the least understood of the group III-nitride compounds. The relatively recent discovery that the energy gap of this material is only 0.7 eV,[10] rather than the previously accepted 1.9 eV, has generated a great interest in InN for applications such as high-efficiency solar cells, light-emitting diodes, laser diodes, and high-frequency transistors.[11] Here, we are presenting our first results on the incorporation of As in InN. The layers were grown by PA-MBE on Pyrex substrates at low temperatures. InN layers grown without any As flux show polycrystalline RHEED during growth and polycrystalline XRD after the growth. Even small As fluxes with BEP above 10^{-8} Torr

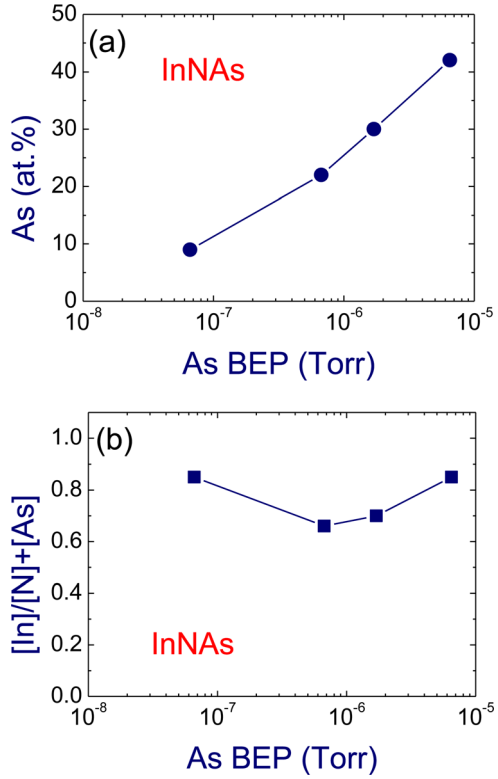

FIG. 5. (Color online) Arsenic concentration (a) and In/(N + As) concentration ratio (b) in the InNAs layers measured by RBS as a function of the As flux during PA-MBE.

suppressed the crystalline growth and the layers became amorphous, in a manner that was very similar to the behavior of the GaN-based HMAs described above.

Figure 5(a) shows RBS measured composition for the $InN_{1-x}As_x$ layers grown under different As fluxes at the growth temperatures ~250 °C. Arsenic incorporation gradually increases up to ~40 at. % with increasing As flux. The Group III(In)/Group V(N plus As) concentrations ratio for As doped InN layers are ~0.8 and relatively independent of the As flux [Fig. 5(b)]. Therefore, we probably have a deficiency of In in the $InN_{1-x}As_x$ layers. The In–As bond energy (1.55 eV/bond[9]) is weaker than the In–N bond energy (1.93 eV/bond[9]) but not as different as for Ga–Sb and Ga–N described above. Unfortunately, we were not able to measure any optical properties on these sets of $InN_{1-x}As_x$ layers, because strong absorption occurs in Pyrex substrates, within the optical gap range for the InNAs HMAs. Therefore, we need to repeat the growth on sapphire in order to study the optical properties of $InN_{1-x}As_x$ alloys. However, our preliminary study on MBE of $InN_{1-x}As_x$ layers already shows that the mechanisms of incorporation of group V elements in HMAs during PA-MBE growth are similar for GaN-based and InN-based alloys.

IV. SUMMARY AND CONCLUSIONS

We have presented our first results on the MBE growth and structural and optical characterization of N-rich $GaN_{1-x}Sb_x$ and N-rich $InN_{1-x}As_x$ alloys and compare these with $GaN_{1-x}As_x$ and $GaN_{1-x}Bi_x$ alloys. There are general

similarities in the growth and the properties of N-rich HMAs. The incorporation of As, Sb, and Bi can be enhanced by growing the layers at extremely low growth temperatures. HMAs layers become amorphous for high As, Sb, and Bi content. Although layers become amorphous for high group V anion content, optical absorption measurements show a progressive shift of the optical absorption edge to lower energy. The results strongly suggest that amorphous HMAs layers have short-range order resembling random crystalline HMAs. The large band gap range and controllable conduction and valence band positions of these HMAs make them promising materials for efficient solar energy conversion devices. The amorphous nature of the HMAs is particularly advantageous since low cost substrates such as glass can be used for solar cell fabrication.

ACKNOWLEDGMENTS

The MBE growth at the University of Nottingham and characterization at the University of Strathclyde were undertaken with support from the EPSRC. Material characterization work performed at LBNL was supported by the Director, Office of Science, Office of Basic Energy Sciences, Materials Sciences and Engineering Division, of the U.S. Department of Energy under Contract No. DE-AC02-05CH11231.

[1]J. Wu, W. Walukiewicz, K. M. Yu, J. D. Denlinger, W. Shan, J. W. Ager, A. Kimura, H. F. Tang, and T. F. Kuech, Phys. Rev. B **70**, 115214 (2004).
[2]W. Walukiewicz, K. Alberi, J. Wu, W. Shan, K. M. Yu, and J. W. Ager III, in *Physics of Dilute III-V Nitride Semiconductors and Material Systems: Physics and Technology*, edited by A. Erol (Springer-Verlag, Berlin, 2008), Chap. 3.
[3]R. M. Sheetz, E. Richter, A. N. Andriotis, S. Lisenkov, C. Pendyala, M. K. Sunkara, and M. Menon, Phys. Rev. B **84**, 075304 (2011).
[4]S. V. Novikov *et al.*, J. Vac. Sci. Technol. B **28**, C3B12 (2010).
[5]K. M. Yu *et al.*, J. Appl. Phys. **106**, 103709 (2009).
[6]S. V. Novikov *et al.*, Phys. Status Solidi A **209**, 419 (2012).
[7]A. X. Levander *et al.*, J. Mater. Res. **26**, 2887 (2011).
[8]B. Heying, R. Averbeck, L. F. Chen, E. Haus, H. Riechert, and J. S. Speck, J. Appl. Phys. **88**, 1855 (2000).
[9]W. A. Harrison, *Electronic Structure and the Properties of Solids* (W.H. Freeman and Company, San Francisco, 1980), p. 176.
[10]J. Wu, W. Walukiewicz, K. M. Yu, J. W. Ager III, E. E. Haller, H. Lu, W. J. Schaff, and Y. Nanishi, Appl. Phys. Lett. **80**, 3967 (2002).
[11]*Indium Nitride and Related Alloys*, edited by T. D. Veal, C. F. McConville, and W. J. Schaff (CRC, Boca Raton, FL, 2010).